

Sub-Auroral Polarization Streams: A complex interaction between the magnetosphere, ionosphere, and thermosphere

Joachim Raeder¹, William D. Cramer¹, Joseph Jensen¹, Timothy Fuller-Rowell², Naomi Maruyama², Frank Toffoletto³, Hien Vo³

¹Space Science Center, University of New Hampshire, Durham, NH 03824, USA

²CIRES, University of Colorado, Boulder, CO 80303, USA

³Rice University, Houston, TX 77005, USA

⁴Universidad del Turabo, PR

E-mail: J.Raeder@unh.edu

Abstract. We use a novel coupled model of the magnetosphere-ionosphere-thermosphere system consisting of the OpenGGCM magnetosphere model, the CTIM ionosphere-thermosphere model, and the RCM model for the drift physics of the inner magnetosphere to study Sub-Auroral Polarization Streams (SAPS). We use the model to simulate the March 17, 2013 “St. Patrick’s day” geomagnetic storm. It had been previously established that SAPS occur during this storm. We demonstrate that the model can reproduce the salient features of SAPS. In particular, the model reproduces the strong northward electric field associated with westward flows, well equatorward of the convection cells. The flows are located just equatorward of the lower boundary of electron precipitation and thus in a region of low ionosphere conductance. Associated with the flows is a deepening through in electron density. The SAPS extend from post-noon to post-midnight, and with increasing local time they extend to lower and lower latitudes. This had been previously found in a statistical sense, but the model finds that this behavior is also true at given times. We thus conclude that self-consistent modeling of SAPS is now possible, which enables us to study their properties in more detail.

1. Introduction

Sub-auroral Polarization Streams [SAPS] are a feature of the ionosphere that develops mostly during geomagnetic active times [Foster *et al.*, 2007].

Foster and Vo [2002] have shown that SAPS statistically occur primarily in the afternoon sector and that they are more intense as geomagnetic activity increases. The primary characteristics of SAPS is an intense northward electric field that is well equatorward of the convection pattern. This electric field channel is a few degrees wide and can have peak values around 100 mV/m. This corresponds to plasma drift velocities of ~ 2000 m/s. Along with the high speed flow channel, the mid-latitude trough in the electron density deepens. Coincident measurements of electric field, field-aligned currents (FACs), and particle precipitation show that the SAPS electric field is located equatorward of plasma sheet electron precipitation overlapping with region-2 (R2) FAC. Because of the lack of sufficient precipitation, the ionosphere conductance is low. This leads to the simple conjecture that the strong SAPS electric field occurs because the magnetosphere imposes the current, which in a simple electrical circuit



picture requires an increased voltage, i.e., stronger electric field, to support that current. At the same time, increased recombination decreases the ionosphere electron content, which further decreases ionosphere conductance [Rodger, 2008].

An increase of the relative flow velocity between the ions and the neutrals from 1000 km/s to 2000 km/s increases the recombination rate by about an order of magnitude [Schunk *et al.*, 1976]. Thus, there is possibly a positive feedback loop that may enhance the SAPS effect. However, this picture depends on assumptions, for example, that the magnetosphere is a current generator, and that the electron depletion occurs at altitudes where it has a significant effect on conductance.

Even though a rather straight-forward theory may suffice to explain SAPS, at least in a climatological sense, it is quite difficult to model them self-consistently, in particular during geomagnetically active times. Although SAPS are primarily a ionosphere phenomenon, they are driven by the magnetosphere that produces the FAC and electron precipitation, and they require fully three-dimensional modeling of the ionosphere-thermosphere (IT) system. Furthermore, R2 currents are believed to be driven by pressure gradients in the inner magnetosphere, which require the inclusion of the proper drift physics that produces the ring current. In the past each of these systems has been modeled separately, for example CTIM exists as a stand-alone model [Fuller-Rowell *et al.*, 1996], MHD based magnetosphere models exist for a few decades now [Raeder, 2003; Lyon *et al.*, 2004; Toth *et al.*, 2005]. Likewise, models of the inner magnetosphere alone have been used for a long time [Toffoletto *et al.*, 2003; Fok *et al.*, 2001; Jordanova, 2003; Kozyra *et al.*, 1998]. Pairwise coupled models are now common, such as OpenGGCM-CTIM [Raeder *et al.*, 2001a], or coupled models of the inner and outer magnetosphere [Toffoletto *et al.*, 2004; Hu *et al.*, 2010], as well as models of the coupled inner magnetosphere-IT system [Maruyama *et al.*, 2007]. However, coupled simulations with full feedbacks between all of the outer magnetosphere, inner magnetosphere, and the IT systems are relatively new and have not yet been extensively tested.

Here, we present first results from one such model, i.e., the coupled OpenGGCM (magnetosphere), CTIM (IT system), and Rice Convection Model (RCM, inner magnetosphere). As one of the first significant results of that model we show that it can produce the salient features of SAPS.

2. The OpenGGCM-CTIM-RCM Model

The OpenGGCM is a global coupled model of Earth’s magnetosphere, ionosphere, and thermosphere. The magnetosphere part solves the MHD equations as an initial-boundary-value problem. The MHD equations are only solved to within $\sim 3 R_E$ of Earth. The region within $3 R_E$ is treated as a magnetosphere-ionosphere (MI) coupling region where physical processes that couple the magnetosphere to the ionosphere-thermosphere system are parameterized using simple models and relationships. Important for this investigation, we use MHD plasma parameters at the inner boundary to compute electron precipitation parameters, such as the electron energy flux and mean energy associated with diffuse and the discrete aurora. Details of these calculations can be found in Raeder *et al.* [1998, 2001b]; Raeder [2003]; Raeder *et al.* [2008b].

The ionosphere-thermosphere system is modeled using the NOAA CTIM (Coupled Thermosphere Ionosphere Model) [Fuller-Rowell *et al.*, 1996]. The original coupling between the OpenGGCM and CTIM is described in Raeder *et al.* [2001a].

The inner magnetosphere is modeled using the Rice Convection Model [Toffoletto *et al.*, 1996]. Some early results of the coupling between OpenGGCM and RCM were presented by Hu *et al.* [2010]. The coupling of these models has since been improved. Since the domains of the OpenGGCM and the RCM overlap, there exist two computed states of the plasma in that region. Because the RCM description is considered to be more adequate for the physics in this region, i.e., based on the energy dependent drifts, the RCM plasma density and pressure is used

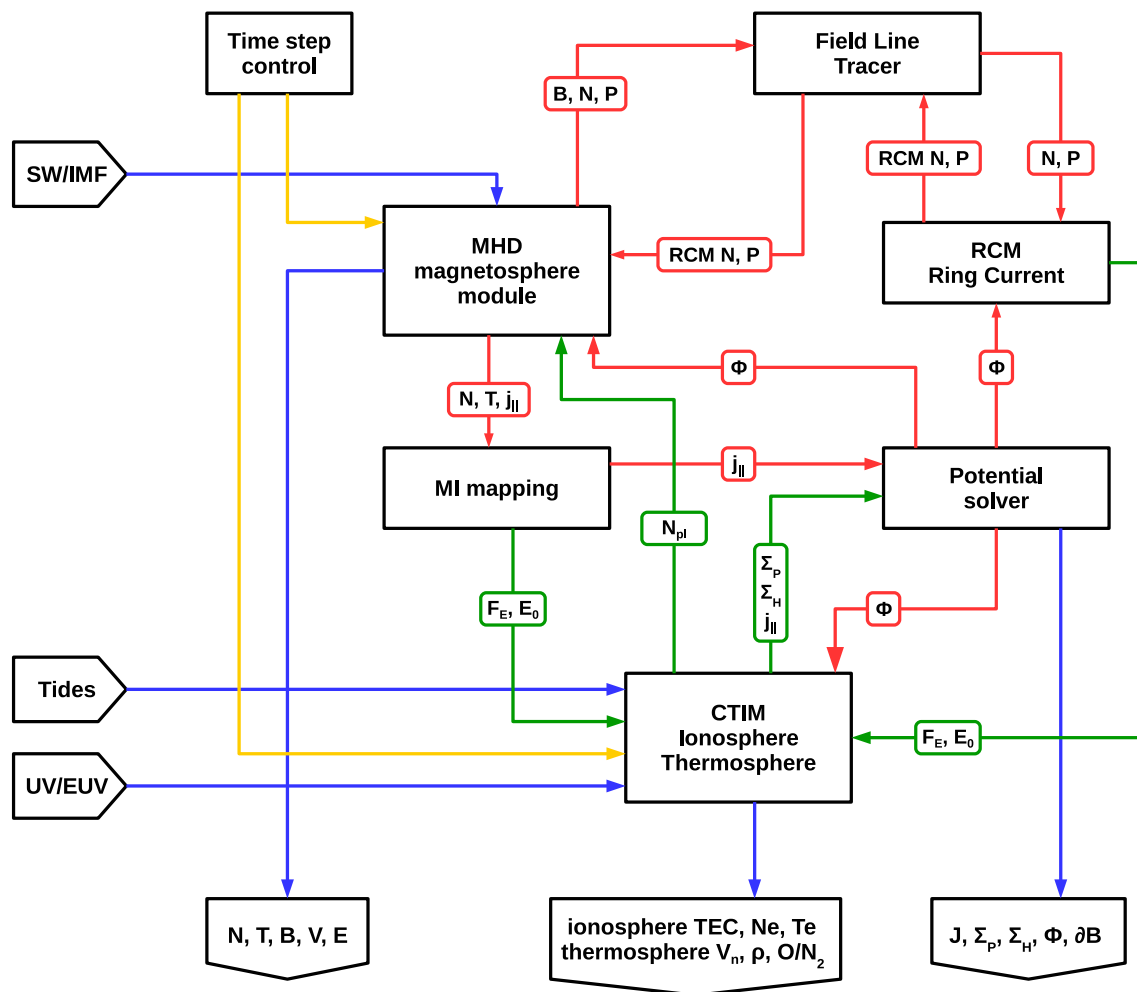


Figure 1. Block diagram of the OpenGGCM with its models and with data/control flow. Blue lines denote model input and output. Red lines denote data flow with strong coupling. Green lines denote data flow with weak or slow coupling. Orange lines denote control flow. B , N , and T are the magnetospheric magnetic field, plasma density, and temperature, respectively. The field aligned current is j_{\parallel} , Φ is the ionosphere potential, F_E and E_0 the energy flux and mean energy of precipitating electrons, Σ_H and Σ_P the ionosphere Hall and Pedersen conductances, and ∂B is the ground magnetic perturbation.

to override the MHD values. However, a simple overwrite feature will not work properly and is thus replaced by a blending algorithm that on a reasonable time scale guarantees that the MHD quantities follow the RCM quantities closely. In the region of overlap, the RCM also provides the electron precipitation for the IT system, which is otherwise, i.e., at high latitudes, provided by the MHD solution. In return, the MHD part of the code provides plasma boundary conditions for the RCM, and the electric potential that the RCM uses to calculate the $\mathbf{E} \times \mathbf{B}$ drift. The models are thus tightly coupled, and it can be demonstrated that the coupled model produces much more realistic R2 currents and inner magnetosphere shielding. OpenGGCM has in the past used for numerous studies, such as magnetopause reconnection [Berchem *et al.*, 1995a, b; Raeder, 2006], the plasma depletion layer [Wang *et al.*, 2003, 2004], plasma entry due to double lobe reconnection [Li *et al.*, 2005, 2008, 2009], ballooning modes [Zhu *et al.*, 2009; Raeder *et al.*, 2010, 2012], interplanetary shock impacts [Oliveira and Raeder, 2014; Oliveira *et al.*, 2016], and

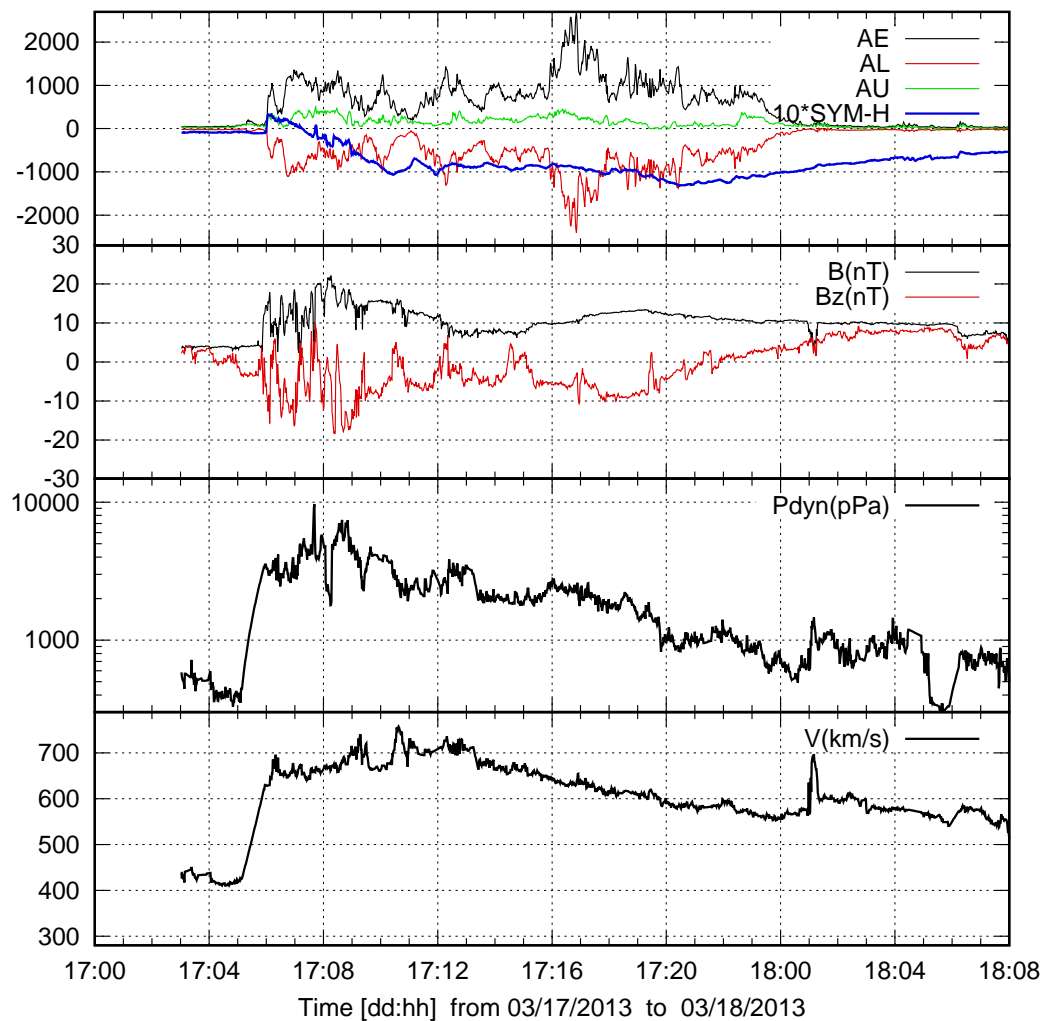


Figure 2. Solar wind, IMF, and geomagnetic conditions on March 17, 2013. The figure shows, from top to bottom: the geomagnetic indices AE, AU, AL, and SYM-H, derived from SuperMAG data; the IMF B_z component, and the field magnitude; the solar wind dynamic pressure; and the solar wind velocity. Note that SYM-H has been multiplied by 10 to fit on the same scale.

substorms [Raeder, 1995; Raeder *et al.*, 2001b; Ge *et al.*, 2011]. A more detailed description of the code and the methods used can be found in Raeder [2003]; Raeder *et al.* [2008a]. The OpenGGCM is available as a community model at the Community Coordinated Modeling Center (CCMC, ccmc.gsfc.nasa.gov), where it also has undergone a number of metrics evaluation studies [Pulkkinen *et al.*, 2010, 2011, 2013; Rastätter *et al.*, 2013]. Here, we demonstrate that the coupled model also produces SAPS.

3. SAPS event

The March 17, 2013 (St. Patrick’s Day) storm event was chosen by the GEM and CEDAR communities for coordinated studies. It has been shown that during this event intense SAPS

occurred [*Foster et al.*, 2014], which also led to the large-scale circulation of plasma to high latitudes and the convection throat. This leads to the formation of a Storm-Enhanced Density (SED) feature, and the so-called Tongue Of Ionization (TOI). However, in this paper, we will not address these phenomena and focus on SAPS.

The March 17 storm was caused by an Interplanetary Coronal Mass Ejection (ICME) that impinged on the magnetosphere. Figure 2 shows solar wind and Interplanetary Magnetic Field (IMF) data for that event. The storm commenced around 0600 UT on March 17, with a sudden increase in solar wind speed, dynamic pressure, and IMF magnitude. Initially, the IMF B_z fluctuated between southern and northern directions, until it turned mostly southward around 0900 UT. It stayed mostly southward until ~ 2000 UT. In the later phase of the storm B_z slowly and smoothly turned northward, indicating that the field represented an ICME flux rope. The SYM-H index fell gradually from the commencement of the storm at ~ 0600 UT to -100 nT at 0900 UT, and then stayed essentially constant until the beginning of the recovery at ~ 2100 UT. The storm is thus quite typical, and of weak to moderate strength. AE values during the storm are typically around 1000 nT, except for a burst of activity starting at ~ 1600 UT, where AE reaches values of up to 2000 nT

4. SAPS development

This storm was previously modeled using the Space Weather Modeling Framework [*Yu et al.*, 2015]. Their model also includes the outer magnetosphere, inner magnetosphere, and ionosphere, but lacks a dynamic and self-consistent ionosphere-thermosphere model. It uses an empirical model for ionosphere conductance, which may lead to missing the critical relation between R2 currents and conductance. Furthermore, there is no feedback from the inner magnetosphere model to the MHD solution. That model thus produces at best hints of SAPS with drift speeds of a few 100 m/s, whereas the observations show speeds of the order of 2000 km/s. (see Figure 8 in *Yu et al.* [2015].)

The OpenGGCM results are presented in Figures 3-5. Each figure shows a polar view of the northern hemisphere. There are four panels in each figure. Panel (A) shows the northward component of the electric field, i.e., E_θ in polar solar magnetic (SM) coordinates. Comparison to drift speeds is facilitated by noting that 50 mV/m correspond to ~ 1000 m/s drift speed. Panel (B) shows the diffuse electron precipitation energy flux. This flux is computed from the thermal energy flow from magnetospheric electrons, assuming a full loss cone. It essentially represents the auroral oval. Panel (C) shows the vertical Total Electron Content (TEC), as computed in CTIM. Panel (D) shows the ionosphere Pedersen conductance, computed self-consistently in CTIM from electron density, neutral densities, and collision frequencies. Obviously, the nightside conductance is closely related to precipitation.

Figure 3 shows the ionosphere state at 0736 UT, shortly after storm commencement. At this time, the dawn electric field has already intensified. The corresponding flow channel stretches from noon MLT to past midnight. The strong electric field is clearly separated, and equatorward of, the precipitation shown in panel (B). However, part of the channel is still on open field lines (the open-closed boundary is shown by the red line), thus, the afternoon portion of the flow should probably not be labeled SAPS. However, in the evening and night side, the flows are clearly separated from the polar cap. Furthermore, past 2000 MLT the flows split into two channels, a feature that is often observed with SAPS. Such separation is visible in the data as shown in the *Yu* paper (see Figure 8 in *Yu et al.* [2015].) Panel (C) shows that at this time no trough has formed yet, except maybe for a hint of depletion around dusk. It appears that at this time TEC in that region is still dominated by auroral electron precipitation.

Figure 4 shows, in the same format as Figure 3, the northern polar ionosphere at 1024 UT. By this time the SAPS is fully developed. Specifically, the flow channel now extends from ~ 1400 UT to past midnight and is well separated from the polar cap and from the precipitation region.

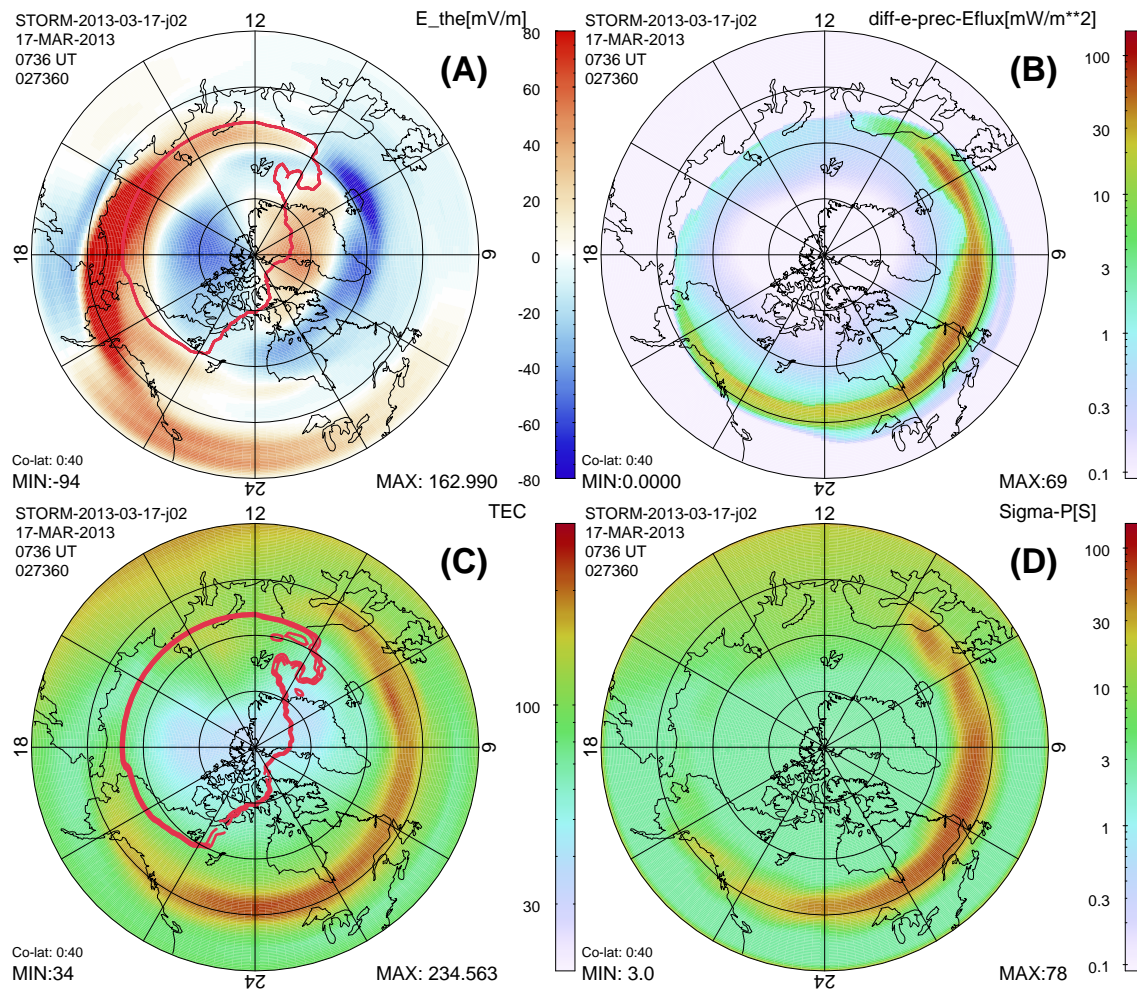


Figure 3. State of the ionosphere at 0736 UT. Polar views of (A) northward component of the northward component (B_θ in polar SM coordinates) ionosphere electric field, (B) diffuse electron precipitation, (C) the vertical Total Electron Content (TEC), and (D) the Pederen conductance. Each figure covers 50° latitude to the pole, and circles are drawn every 10 degrees.

Nearly coincident, a trough has developed and deepened in TEC. The trough is rotated some 2-3 hours local time past the flows, because the flow channel is stationary in the SM frame, whereas the electrons tend to co-rotate with the Earth, i.e., they are more stationary in the geographic frame. The trough thus extends substantially past midnight. A trough-like feature also begins to show in the conductance. It is also noteworthy that the latitude of the flow channel has a MLT dependence, such that the channel is at lower latitude as MLT increases. This has previously been found in statistical studies [Foster and Vo, 2002]. The simulation shows that such dependence can also exist at any given time.

Figure 5 shows the ionosphere at 1528 UT. This is still during the main phase of the storm; however, as Figure 2 shows, just after a brief phase of northward IMF. The SAPS now show some signs of recovery. The electric field is weaker, and the trough starts to disappear on the dayside, but still keeps co-rotating. Also, the flow channel progresses to lower latitudes in the night side. The SYM-H index (essentially the same as Dst) does not correlate well with SAPS development, since it reacts slowly to IMF changes. Likewise, the A-indices only seem to correlate weakly with SAPS as they primarily describe the high-latitude disturbances. Apparently, the SAPS electric

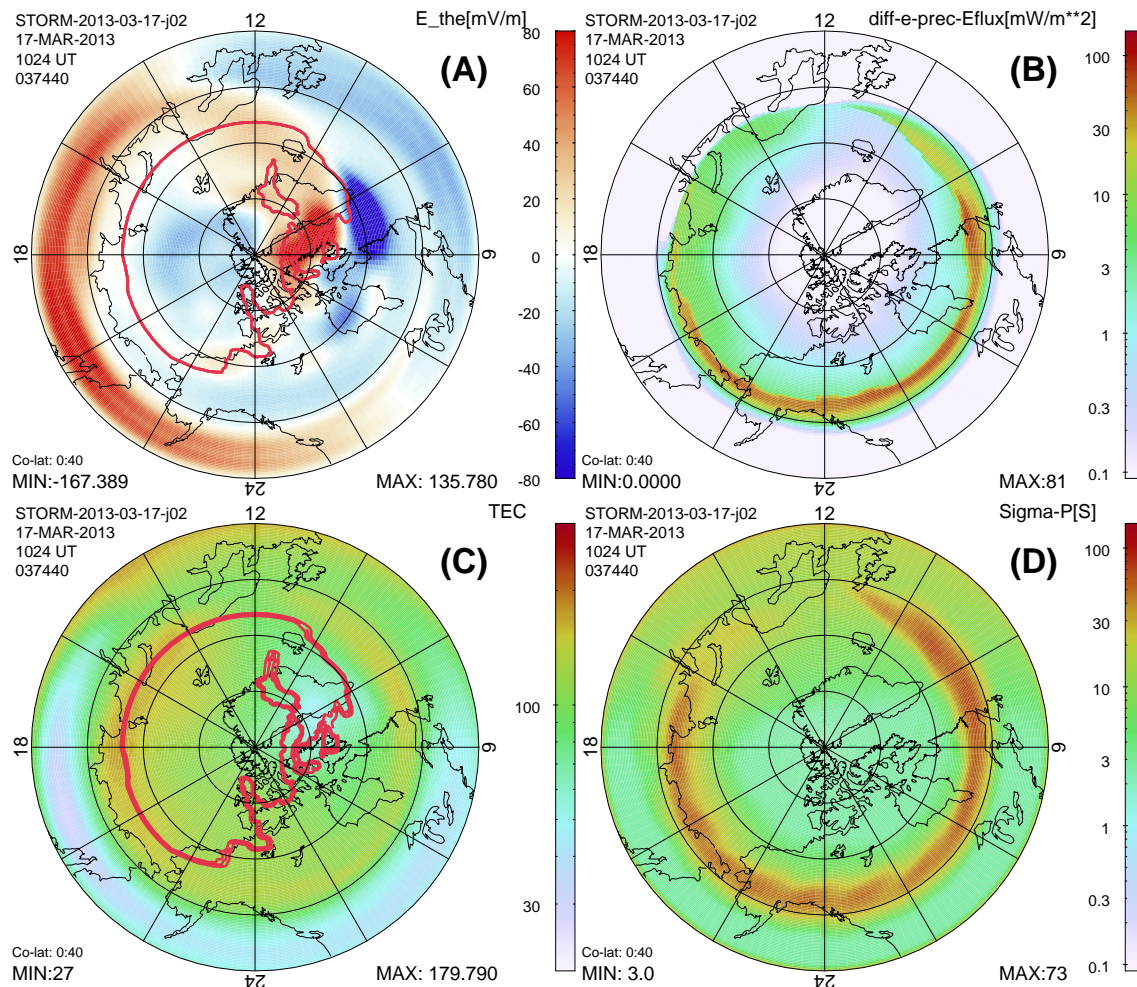


Figure 4. State of the ionosphere at 1024 UT, in the same format as Figure 3.

field reacts much more quickly to IMF changes, although the driver, i.e., the inner magnetosphere pressure distribution that drives the R2 currents is related to SYM-H. This warrants further investigation.

5. Summary and conclusions

We have presented a new model, consisting of the OpenGGCM for the outer magnetosphere, the RCM for the inner magnetosphere, and CTIM for the ionosphere-thermosphere system. We used the model to simulate the March 17, 2013 geomagnetic storm, which had previously been investigated and shown to develop significant SAPS.

We show that the model reproduces the salient features of SAPS, namely the strong northward fields and associated ion drifts, and the coincident trough in electron density. These features follow largely the characteristics established by statistical studies, i.e., the magnitude of the flows, and their latitude dependence on MLT. Also, as established in previous work, the model shows that the SAPS fields are well separated from the convection pattern itself, and that they lie equatorward of regions of electron precipitation.

Although fairly comprehensive data are available for this event, we forgo a detailed comparison, which is beyond the scope of this paper. We note, however, that a simple eye-

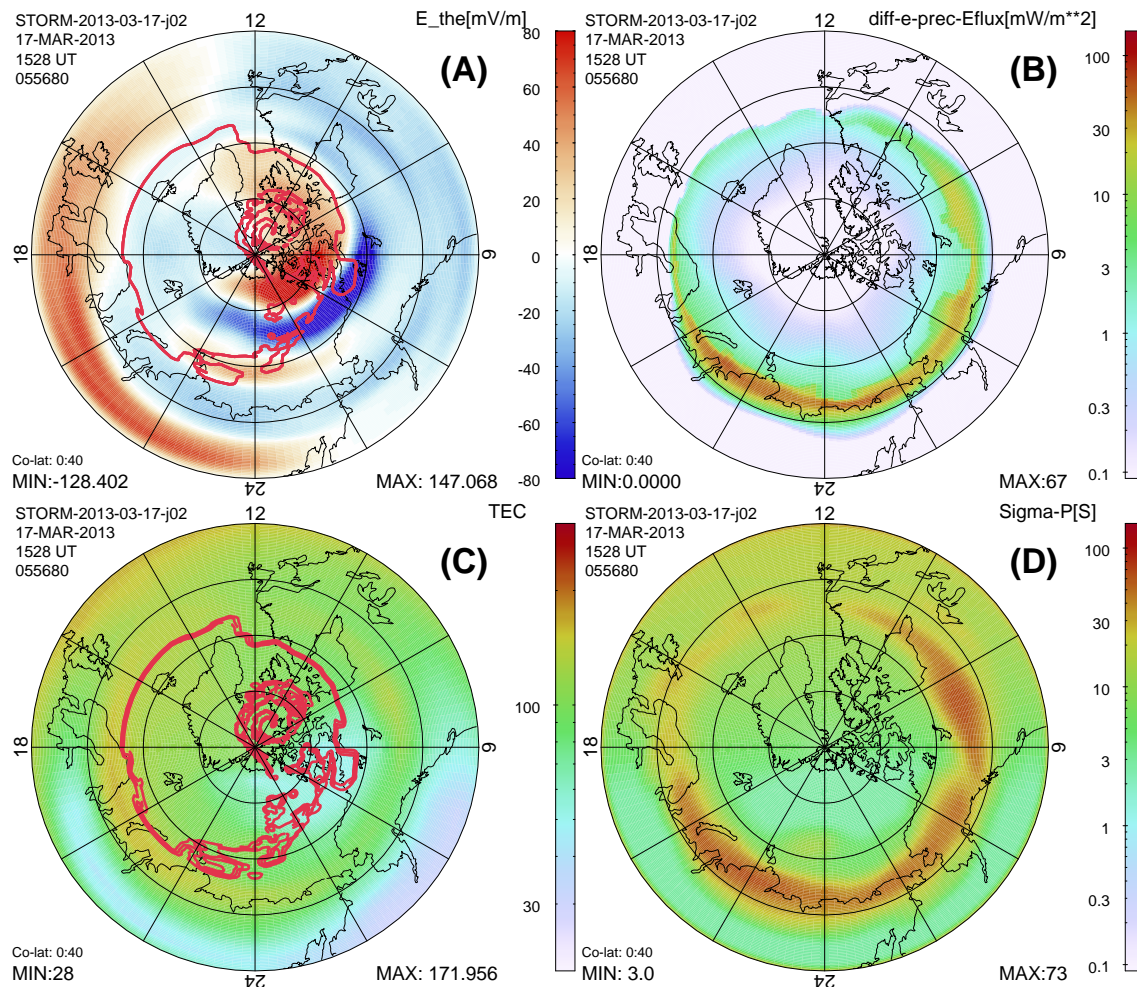


Figure 5. State of the ionosphere at 1538 UT, in the same format as Figure 3.

balling comparison with the DMSP passes presented in the *Yu et al.* [2015] paper reveals that the SAPS electric field and flow speed values in our model, which reach some 100 mV/m and 2000 km/s, respectively, compare well with the data.

We contrast this with the results of the *Yu* paper, which shows much weaker flows. The reason for this may be the fact that their model does not include a self-consistent ionosphere-thermosphere model to produce the ionosphere conductance, whereas ours does. Indeed, we observe in our results the development of a deep trough in the electron density, which lowers the conductance. Thus, our results indicate that the positive feedback between the flows, electron density, and conductance may be critical for development of SAPS, as indicated in the *Rodger* [2008] review, for example. We will investigate this in forthcoming studies by comparing with model runs that quench the feedback, and by comparing with data.

Acknowledgments

JR would like to thank J. Foster, P. Erickson, and P. Anderson for enlightening discussions. For the ground magnetometer data we gratefully acknowledge the SuperMAG contributors and PI Jesper Gjerloev, funded under NSF ATM-0646323, NSF AGS-1003580, and NASA NNX08AM32G S03. The work at UNH was funded through grant AGS-1143895 from the

National Science Foundation, and NASA/LWS grant NNX13AK31G. Computations were performed on Trillian, a Cray XE6m-200 supercomputer at UNH supported by the NSF MRI program under grant PHY-1229408.

References

- Berchem, J., J. Raeder, and M. Ashour-Abdalla, Reconnection at the magnetospheric boundary: Results from global MHD simulations, in *Physics of the Magnetopause*, edited by B. U. Sonnerup and P. Song, vol. 90 of *AGU Geophysical Monograph*, p. 205, 1995a.
- Berchem, J., J. Raeder, and M. Ashour-Abdalla, Magnetic flux ropes at the high-latitude magnetopause, *Geophys. Res. Lett.*, *22*, 1189, 1995b.
- Fok, M.-C., R. A. Wolf, R. W. Spiro, and T. E. Moore, Comprehensive computational model of the Earth's ring current, *J. Geophys. Res.*, *106*, 8417, 2001.
- Foster, J. C., and H. B. Vo, Average characteristics and activity dependence of the sub auroral polarization stream, *J. Geophys. Res.*, *107*, doi:10.1029/2002JA009409, 2002.
- Foster, J. C., W. Rideout, B. Sandel, W. T. Forrester, and F. J. Rich, On the relationship of SAPS to storm-enhanced densities, *J. Atm. Sol. Terr. Phys.*, *69*, 303, 2007.
- Foster, J. C., P. J. Erickson, A. J. Coster, S. Thaller, J. Tao, J. R. Wygant, and J. W. Bonnell, Storm time observations of plasmasphere erosion flux in the magnetosphere and ionosphere, *Geophys. Res. Lett.*, *41*, 762–768, 2014.
- Fuller-Rowell, T. J., D. Rees, S. Quegan, R. J. Moffett, M. V. Codrescu, and G. H. Millward, A coupled thermosphere-ionosphere model (CTIM), in *STEP Report*, edited by R. W. Schunk, p. 217, Scientific Committee on Solar Terrestrial Physics (SCOSTEP), NOAA/NGDC, Boulder, Colorado, 1996.
- Ge, Y. S., J. Raeder, V. Angelopoulos, M. L. Gilson, and A. Runov, Interaction of dipolarization fronts within multiple bursty bulk flows in global MHD simulations of a substorm on 27 February 2009, *J. Geophys. Res.*, *116*, A00I23, 2011.
- Hu, B., F. Toffoletto, S. Sazykin, J. Raeder, D. Larson, and A. Vapirev, RCM simulation of the March 23rd 2007 substorm event using the OpenGGCM, *J. Geophys. Res.*, *115*, A12,205 doi:10.1029/2010JA015360, 2010.
- Jordanova, V. K., New insights of geomagnetic storms from model simulations using multi-spacecraft data, *Space Science Reviews*, *107*, 157, 2003.
- Kozyra, J. U., V. K. Jordanova, J. E. Borovsky, M. F. Thomsen, D. J. Knipp, D. S. Evans, D. J. McComas, and T. E. Cayton, Effects of a high-density plasma sheet on ring current development during the november 2-6, 1993, magnetic storm, *Journal of Geophysical Research*, *103*, 26,285–305, 1998.
- Li, W., J. Raeder, J. Dorelli, M. Øieroset, and T. D. Phan, Plasma sheet formation during long period of northward IMF, *Geophys. Res. Lett.*, *32*, L12S08, doi: 10.1029/2004GL021524, 2005.
- Li, W., J. Raeder, J. C. Dorelli, M. Thomsen, and B. Lavraud, Solar wind entry into the magnetosphere under northward IMF conditions, *J. Geophys. Res.*, *113*, A04,204, 2008.
- Li, W., J. Raeder, M. Øieroset, and T. D. Phan, Cold dense magnetopause boundary layer under northward IMF: Results from THEMIS and MHD simulations, *J. Geophys. Res.*, *114*, A00C15, doi:10.1029/2008JA013497, 2009.
- Lyon, J. G., J. A. Fedder, and C. M. Mobarry, The Lyon-Fedder-Mobarry (LFM) global MHD magnetospheric simulation code, *J. Atm. Sol. Terr. Phys.*, *66*, 1333, 2004.
- Maruyama, N., et al., Modeling storm-time electrodynamics of the low-latitude ionosphere–thermosphere system: Can long lasting disturbance electric fields be accounted for?, *J. Atm. Sol. Terr. Phys.*, *69*, 1182–1199, 2007.
- Oliveira, D. M., and J. Raeder, Impact angle control of interplanetary shock geoeffectiveness, *J. Geophys. Res.*, *119*, 8188, 2014.
- Oliveira, D. M., J. Raeder, B. T. Tsurutani, and J. W. Gjerloev, Effects of interplanetary shock inclinations on nightside auroral power, *Braz. Jour. Phys.*, *46*, 97–104, 2016.
- Pulkkinen, A., L. Rastätter, K. Kuznetsova, M. Hesse, A. Ridley, J. Raeder, H. J. Singer, and A. Chulaki, Systematic evaluation of ground and geostationary magnetic field predictions generated by global magnetohydrodynamic models, *J. Geophys. Res.*, *115*, A03,206, 2010.

- Pulkkinen, A., et al., Geospace environment modeling 2008-2009 challenge: Ground magnetic field perturbations, *Space Weather*, *9*, S02,004, 2011.
- Pulkkinen, A., et al., Community-wide validation of geospace model ground magnetic field perturbation predictions to support model transition to operations, *Space Weather*, *11*, 369 doi:10.1002/swe.20,056, 2013.
- Raeder, J., Global MHD simulations of the dynamics of the magnetosphere: Weak and strong solar wind forcing, in *Proceedings of the Second International Conference on Substorms*, edited by J. R. Kan, J. D. Craven, and S.-I. Akasofu, p. 561, Geophysical Institute, Univ. of Alaska Fairbanks, 1995.
- Raeder, J., Global Magnetohydrodynamics – A Tutorial, in *Space Plasma Simulation*, edited by J. Büchner, C. T. Dum, and M. Scholer, Springer Verlag, Berlin Heidelberg New York, 2003.
- Raeder, J., Flux transfer events: 1. Generation mechanism for strong southward IMF, *Ann. Geophys.*, *24*, 381, 2006.
- Raeder, J., J. Berchem, and M. Ashour-Abdalla, The Geospace Environment Modeling grand challenge: Results from a Global Geospace Circulation Model, *J. Geophys. Res.*, *103*, 14,787, 1998.
- Raeder, J., Y. L. Wang, and T. J. Fuller-Rowell, Geomagnetic storm simulation with a coupled magnetosphere - ionosphere - thermosphere model, in *Space Weather, AGU Geophys. Monogr. Ser.*, edited by P. Song, G. Siscoe, and H. J. Singer, vol. 125, p. 377, American Geophysical Union, 2001a.
- Raeder, J., D. Larson, W. Li, E. L. Kepko, and T. Fuller-Rowell, OpenGGCM simulations for the THEMIS mission, *Space Sci. Rev.*, *141*, 535, doi:10.1007/s11,214-008-9421-5, 2008a.
- Raeder, J., D. Larson, W. Li, E. L. Kepko, and T. Fuller-Rowell, OpenGGCM simulations for the THEMIS mission, *Space Sci. Rev.*, *141*, 535, 2008b.
- Raeder, J., P. Zhu, Y. Ge, and G. L. Siscoe, OpenGGCM simulation of a substorm: Axial tail instability and ballooning mode preceding substorm onset, *J. Geophys. Res.*, *115*, A00116, 2010.
- Raeder, J., P. Zhu, and Y. Ge, Auroral signatures of ballooning mode near substorm onset: OpenGGCM simulations, in *Auroral Phenomenology and Magnetospheric Processes: Earth and other Planets*, edited by A. Keiling, E. Donovan, F. Bagenal, and T. Karlsson, vol. 197 of *AGU Geophysical Monograph*, pp. 389–395, 2012.
- Raeder, J., et al., Global simulation of the geospace environment modeling substorm challenge event, *J. Geophys. Res.*, *106*, 381, 2001b.
- Rastätter, L., et al., Geospace environment modeling 2008 - 2009 challenge: Dst index, *Space Weather*, *11*, 187–205, 2013.
- Rodger, A., The mid-latitude trough—revisited, in *Midlatitude Ionospheric Dynamics and Disturbances*, pp. 25–33, Wiley-Blackwell, 2008.
- Schunk, R. W., P. M. Banks, and W. J. Raitt, Effects of electric fields and other processes upon the nighttime high-latitude F layer, *J. Geophys. Res.*, *81*, 3271–3282, 1976.
- Toffoletto, F. R., R. W. Spiro, R. A. Wolf, M. Hesse, and J. Birn, Self-consistent modeling of inner magnetospheric convection, in *Third International Conference on Substorms (ICS-3)*, edited by E. J. Rolfe and B. Kaldeich, p. 223, ESA SP-389, ESA Publications Division, Noordwijk, The Netherlands, 1996.
- Toffoletto, F. R., S. Sazykin, R. W. Spiro, and R. A. Wolf, Modeling the inner magnetosphere using the rice convection model, *Space Sci. Rev.*, *108*, 175, 2003.
- Toffoletto, F. R., S. Sazykin, R. W. Spiro, R. A. Wolf, and J. G. Lyon, RCM meets LFM: initial results of one-way coupling, *J. Atm. Sol. Terr. Phys.*, *66*, 1361, 2004.
- Toth, G., et al., Space weather modeling framework: A new tool for the space science community, *J. Geophys. Res.*, *110*, 21, doi:10.1029/2005JA011,126, 2005.
- Wang, Y. L., J. Raeder, C. T. Russell, T. D. Phan, and M. Manapat, Plasma depletion layer: Event studies with a global model, *J. Geophys. Res.*, *108*, 1010, doi:10.1029/2002JA009,281, 2003.
- Wang, Y. L., J. Raeder, and C. T. Russell, Plasma depletion layer: Structure and forces, *Ann. Geophys.*, *22*, 1001, 2004.
- Yu, Y., V. Jordanova, S. Zou, R. Heelis, M. Ruohoniemi, and J. Wygant, Modeling subauroral polarization streams during the 17 march 2013 storm, *J. Geophys. Res.*, *120*, 1738–1750, 2015.
- Zhu, P., J. Raeder, K. Germaschewski, and C. C. Hegna, Initiation of ballooning instability in the near-Earth plasma sheet prior to the 23 March 2007 THEMIS substorm expansion onset, *Ann. Geophys.*, *27*, 1129, 2009.